DMD Fast Forward. Published on January 7, 2020 as DOI: 10.1124/dmd.119.087338
This article has not been copyedited and formatted. The final version may differ from this version.

Biotransformation Pathways and Metabolite Profiles of Oral [^{14}C]-Alisertib (MLN8237), an Investigational Aurora A Kinase Inhibitor, in Patients with Advanced Solid Tumors

Authors: Sandeepraj Pusalkar, Xiaofei Zhou, Yuexian Li, Lawrence Cohen, Jun Johnny Yang*, Suresh K. Balani, Cindy Xia, Wen Chyi Shyu, Chuang Lu**, Karthik Venkatakrishnan, and Swapan K. Chowdhury

Affiliation: *Millennium Pharmaceuticals, Inc., Cambridge, Massachusetts, USA, a wholly owned subsidiary of Takeda Pharmaceutical Company Limited (S.P., X.Z., Y.L., L.C., J.Y., S.K.B., C.X., W.C.S., C.L. K.V., S.K.C.)*

*Current affiliation: *iHOPE Hill, LLC, Cambridge, MA, 02139, USA; **Department of DMPK, Sanofi USA, 153 Second Avenue, Waltham, MA, 02451, USA.*

Primary Laboratory of Origin:

The study was conducted at a single clinical center in the United States: Comprehensive Clinical Development (Tacoma, Washington). Medical and clinical monitoring, including oversight of study drug packaging, labeling, and shipping, were conducted by the study sponsor: Millennium Pharmaceuticals, Inc., a wholly owned subsidiary of Takeda Pharmaceutical Company Limited (Cambridge, Massachusetts). Plasma and urine samples were shipped from Comprehensive Clinical Development to Frontage Laboratories, Inc. (Exton, Pennsylvania, USA), while fecal homogenates were prepared by Charles River Laboratories (Senneville, Québec City, Canada) and duplicate aliquots then shipped to Frontage Laboratories, Inc. for metabolite profiling.

Running title [**max. 60** characters w/ spaces; currently **60**]:

Alisertib metabolic profile in pts with advanced solid tumor

Corresponding author:

Sandeepraj Pusalkar, PhD

Drug Metabolism and Pharmacokinetics, Millennium Pharmaceuticals, Inc., a wholly owned subsidiary of Takeda Pharmaceutical Company Limited

40 Landsdowne St., Cambridge, MA 02139, USA.

Tel: +1-617-374-7795

Fax: +1-617-444-1501

Email: sandeepraj.pusalkar@takeda.com

Journal: *Drug Metabolism and Disposition*

Number of text pages: 63

Tables / figures (no max specified): 8 / 6

Abstract (max 250 words): 280 words

Introduction (max 750 words): 471 words

Discussion (max 1500 words): 1584 words

References: 38

ABBREVIATIONS: AAK, Aurora A kinase; ACN, acetonitrile; ADME, absorption, distribution, metabolism, and excretion; AUC, area under the plasma/whole blood concentration–time curve; BID, twice daily; CYP, cytochrome P450; DDI, drug-drug interaction; ECT, enteric-coated tablet; HPLC, high-performance liquid chromatography; HPLC/UV/MS, high-performance liquid chromatography with ultraviolet and mass spectrometry detectors; LC/MS/MS, liquid chromatography with tandem mass spectrometry; LSC, liquid scintillation counting; LTQ, linear trap quadropole; NADPH, nicotinamide adenine dinucleotide phosphate; rCYP, recombinant CYP; TRA, total radioactivity; RAF, relative activity factor; UGT, uridine 5'-diphospho-glucuronosyltransferase; UV, ultraviolet

Trial ID: ClinicalTrials.gov #NCT01714947

DMD Fast Forward. Published on January 7, 2020 as DOI: 10.1124/dmd.119.087338
This article has not been copyedited and formatted. The final version may differ from this version.

Abstract

Alisertib (MLN8237) is an investigational, orally available, selective Aurora A kinase inhibitor in clinical development for the treatment of solid tumors and hematological malignancies. This metabolic profiling analysis was conducted as part of a broader phase 1 study evaluating mass balance, pharmacokinetics, metabolism, and routes of excretion of alisertib following a single 35 mg dose of [^{14}C]-alisertib oral solution (~80 µCi) in three patients with advanced malignancies. On average, 87.8% and 2.7% of the administered dose was recovered in feces and urine, respectively, for a total recovery of 90.5% by 14 days post-dose. Unchanged [^{14}C]-alisertib was the predominant drug-related component in plasma, followed by *O*-desmethyl alisertib (M2), and alisertib acyl glucuronide (M1) present at 47.8%, 34.6%, and 12.0% of total plasma radioactivity. In urine, of the 2.7% of the dose excreted, unchanged [^{14}C]-alisertib was a negligible component (trace), with M1 (0.84% of dose) and glucuronide conjugate of hydroxy alisertib (M9; 0.66% of dose) representing the primary drug-related components in urine. Hydroxy-alisertib (M3; 20.8% of the dose administered) and unchanged [^{14}C]-alisertib (26.3% of the dose administered) were the major drug-related components in feces. *In vitro*, oxidative metabolism of alisertib was primarily mediated by CYP3A. The acyl glucuronidation of alisertib was primarily mediated by UGT1A1, 1A3, and 1A8, and was stable in 0.1M phosphate buffer and in plasma and urine. Further *in vitro* evaluation of alisertib and its metabolites M1 and M2 for CYP-based drug-drug interaction (DDI) showed minimal potential for perpetrating DDI with co-administered drugs. Overall, renal elimination played an insignificant role in the disposition of alisertib, and metabolites resulting from phase I oxidative pathways contributed to >58% of the alisertib dose recovered in urine and feces over 192 hours post-dose.

DMD Fast Forward. Published on January 7, 2020 as DOI: 10.1124/dmd.119.087338
This article has not been copyedited and formatted. The final version may differ from this version.

Significance Statement

This study describes the primary clearance pathways of alisertib and illustrates the value of timely conduct of human ADME studies in providing guidance to the clinical pharmacology development program for oncology drugs, for which a careful understanding of sources of exposure variability is crucial to inform risk management for DDIs given the generally limited therapeutic window for anticancer drugs and polypharmacy that is common in cancer patients.

DMD Fast Forward. Published on January 7, 2020 as DOI: 10.1124/dmd.119.087338
This article has not been copyedited and formatted. The final version may differ from this version.

Introduction

Aurora A kinase (AAK) is a member of a family of serine/threonine kinases that play an important role in cellular mitosis (Kitzen, de Jonge, and Verweij, 2010). AAK regulates the formation of mitotic spindle poles, G2/M phase transition, and centrosome maturation (Dar et al., 2010). Previous studies have demonstrated amplification and/or overexpression of AAK in a variety of hematologic and non-hematologic malignancies (Bischoff et al., 1998; Gritsko et al., 2003; Lee et al., 2006; Mazumdar et al., 2009; Park et al., 2008; Rojanala et al., 2004; Wang et al., 2006; Zhang et al., 2008). Inhibition of AAK results in an array of mitotic progression defects, ultimately leading to cell death or mitotic arrest (Glover et al., 1995; Hirota et al., 2003; Hoar et al., 2007; Kaestner, Stolz, and Bastians, 2009; Katayama and Sen, 2010; Marumoto et al., 2003; Sasai et al., 2008); as such, AAK represents an attractive target for anticancer therapy.

Alisertib (MLN8237; sodium 4-{[9-chloro-7-(2-fluoro-6-methoxyphenyl)-5H-pyrimido[5,4-d][2]benzazepin-2-yl]amino}-2-methoxybenzoate hydrate) (Millennium Pharmaceuticals, Inc., Cambridge, Massachusetts, USA) is an investigational, orally available, selective inhibitor of AAK (Sells et al., 2015). The pharmacokinetics, safety, and efficacy of alisertib were evaluated across several phase 1 and 2 clinical trials in patients with advanced cancers (Cervantes et al., 2012; Dees et al., 2012; Matulonis et al., 2012; Falchook et al., 2014; Friedberg et al., 2014; Goldberg et al., 2014; Kelly et al., 2014; Melichar et al., 2015). These studies informed a recommended alisertib dose and schedule of 50 mg twice daily (BID) as an enteric-coated tablet (ECT) formulation for 7 days in 21-day cycles (Cervantes et al., 2012; Dees et al., 2012; Falchook et al., 2014; Kelly et al., 2014; Venkatakrishnan et al,

2015). Alisertib continues to be evaluated as a single agent or in combination across multiple indications.

Data from preclinical studies demonstrated that alisertib is metabolized by both glucuronidation and oxidation pathways. In rats, the major metabolic route of [^{14}C]-alisertib was acyl glucuronidation, with approximately 77.9% of the dose metabolized by this pathway and excreted in bile. In-vivo metabolic profiling studies in rats using [^{14}C]-alisertib showed that unchanged alisertib was the predominant circulating component in plasma, accounting for approximately 93% of the total radioactivity (TRA) in plasma over a 24-hour period (Millennium Pharmaceuticals, Inc., unpublished data). Characterization of the metabolic pathway of alisertib in humans is of importance for understanding how the pharmacokinetic profile of the drug may be affected by patient-specific factors (e.g. renal, hepatic function) or by interactions with other medications (drug-drug interactions). Such knowledge will help guide future clinical evaluation of alisertib, and ultimately assist in informing appropriate dosing for patients with impaired organ function.

This metabolic profiling study was conducted as part of an open-label phase 1 trial that evaluated the mass balance, metabolism, routes of excretion, and pharmacokinetics of oral [^{14}C]-alisertib in patients with advanced malignancies (NCT01714947) (Zhou et al., 2018).

DMD Fast Forward. Published on January 7, 2020 as DOI: 10.1124/dmd.119.087338
This article has not been copyedited and formatted. The final version may differ from this version.

Methods

Patients. Three patients, two of them male, all with solid tumors (stage IV ovarian cancer, stage IV bladder cancer, and mesothelioma of unknown stage; each *n* = 1), were enrolled and treated with alisertib. Two of the three patients were white and the other was black. The mean age was 64 years (50, 66, and 76 years, respectively). The mean weight and body mass index were 80.3 ± 20.8 kg (range, 63.0–103.3 kg) and 26.9 ± 8.3 kg/m² (range, 21.6–36.5 kg/m²), respectively.

Study Design, Objectives, and Treatment. The primary objective of the present analysis was to characterize the metabolic profile of alisertib in plasma, urine, and feces following an oral administration of [^{14}C]-alisertib to define the clearance mechanisms and biotransformation pathways in cancer patients.

Patients were admitted to the clinical facility on the morning preceding the first dose of alisertib (day -1). Following the collection of pre-dose assessments on day 1, three patients received a single 35 mg dose of [^{14}C]-alisertib oral solution containing approximately 80 µCi of total radioactivity (TRA; 1.19 mCi/mmol) (Millennium Pharmaceuticals, Inc., Cambridge, Massachusetts, USA). The actual amount of administered radioactivity was documented for each patient.

Patients were not allowed to have any food, except for water, 2 hours before receiving alisertib and for an additional hour after dosing. Use of antacids or calcium-containing supplements from 2 hours before alisertib dosing until up to 2 hours after was not permitted. Patients drank the alisertib oral solution directly from the vial, followed by 3 x 10 mL rinses with water directly from the vial, and then ingestion of approximately 200 mL of water. On the evening of day 7, patients received 2 x 15 mL doses of oral Milk of Magnesia (magnesium hydroxide) approximately 2 hours

apart to ensure collection of fecal samples before discharge from the clinical facility; if the first dose of Milk of Magnesia was not tolerated, the second dose was not given. Patients were discharged from the clinic on day 11 (maximum day 17) provided that ≥ 80% of the total dose of radioactivity had been collected or the combined excretion of radioactivity in urine and feces had declined to ≤ 1% of the total administered radioactivity for at least two consecutive days.

Assessments. Serial blood samples for preparation of plasma were collected over a 10-day period, starting at pre-dose on day 1, and then at 0.5, 1, 2, 3, 4, 6, 8, 12, 24, 48, 72, 96, 120, 144, 168, 192, 216, and 240 hours post-dose. Urine and fecal samples were collected pre-dose on day 1, in intervals of 0–12 and 12–24 hours post-dose, and thereafter in 24-hour collection intervals up to 240 hours post-dose. Plasma and urine samples were shipped under dry ice from Comprehensive Clinical Development to Frontage Laboratories, Inc. (Exton, Pennsylvania, USA), while fecal homogenates were prepared by Charles River Laboratories (Senneville, Québec City, Canada) and duplicate aliquots then shipped under dry ice to Frontage Laboratories, Inc., for alisertib metabolic profiling.

Radioactivity Determination

Radioactivity concentrations in plasma, urine, and fecal extracts were determined by a Tri-Carb Model 3100 TR liquid scintillation counter (LSC) (Perkin Elmer) using 5 mL of scintillation fluid (Ultima Gold). Samples were routinely assayed with the LSC for 10 min, or until the 2-sigma error was less than or equal to 2%, whichever came first. Quench correction was performed using an external standard method and LSC was pre-calibrated within 3 months of the sample

analysis. The scintillation spectrometer was programmed to automatically subtract instrument background (including counting cocktail) and to convert counts per minute (cpm) to disintegrations per minute (dpm).

Metabolite Profiling and Identification

Plasma. Human plasma samples were pooled from pre-dose to 192 hours post-dose for each subject using the Hamilton method (Hamilton, Garnett, and Klines, 1981) which is designed to create AUC-representative pooled plasma samples. The pooled 0-192 hour samples for each subject were analyzed to obtain metabolite profiles, to identify the major metabolites in circulation, and to determine the relative abundance of radioactive components in human plasma. Further details of plasma volumes taken for pooling can be found in the supplemental material (Supplemental Table 1).

Pooled plasma samples from 0-192 hr per subject were extracted by adding three-volumes of ACN containing 1% formic acid. After mixing, the samples were vortexed and centrifuged at 14000 rpm and 4°C in a Sorvall Super T21 centrifuge for 10 min. The plasma proteins were re-extracted with one-fold volume of ACN containing 1% formic acid, followed by centrifugation at 14000 rpm for 10 min. Proteins were discarded and the supernatants were combined and transferred into clean test tubes and dried completely under a stream of nitrogen. The dried residues were reconstituted with 35% ACN: 65% water prior to analysis.

The extraction efficiency was determined by analyzing duplicate aliquots (15 µL) for radioactivity concentrations by LSC. Aliquots of the supernatants were injected onto the HPLC column. HPLC fractions were collected at 15 second intervals into 96-well Lumaplates (PerkinElmer Life and Analytical Sciences). The

plates were then dried for at least 4 hours in an oven set at 40°C, sealed with a clear plate cover, and then analyzed by a TopCount NXT radiometric microplate reader (PerkinElmer Life and Analytical Sciences). For metabolite identification, supernatants of extracts were analyzed by HPLC/MS/MS method and also co-injected with the metabolite standards.

Urine. Urine was pooled proportionally to their total weight per subject to obtain pooled samples representing approximately 90% of the total radioactivity excreted over the cumulative collection interval (0-192 hr pool) (Zhou et al.). The pooled urine samples (12 mL) were extracted by a solid phase extraction method using a phenomenex Strata C18-E cartridge (55 µM, 70°A, 10g/60 mL). The cartridges were initially washed with doubly distilled water (50 mL) and the drug-related components were subsequently eluted with 50 mL of methanol. The eluent was concentrated under a stream of nitrogen at room temperature. The residues were reconstituted with 1 mL of ACN by vortexing for a few min followed by centrifuging the reconstituted samples at 14000 rpm for 10 min. The supernatants were removed, dried under a stream of nitrogen and reconstituted with 300 µL of 35% ACN: 65% water prior to analysis. The extraction efficiency was determined by analyzing duplicate aliquots (15 µL) for radioactivity concentrations by LSC. For metabolite profiling, aliquots of the supernatants were injected onto the HPLC with UV, and radioactivity detection. For metabolite identification, supernatants of the extracts were analyzed by HPLC/MS/MS method and also co-injected with the metabolite standards.

Feces. Fecal homogenates were pooled proportionally to their total weight across 0-192 hour collection intervals for each subject to obtain pooled samples.

The 0-192 hour sample represented approximately 90% of the total radioactivity excreted in feces over the cumulative collection interval (0-192 hr) (Zhou et al.). The pooled fecal samples (~10 g) were extracted with 3 fold volumes of ACN. After extraction, the samples were vortexed and centrifuged at 14000 rpm and 4°C in a Sorvall Super T21 centrifuge for 10 min. The residues were re-extracted twice with one fold volume of ACN, and then centrifuged at 14000 rpm for 10 min. Solid residues were discarded and the supernatants were combined and transferred into clean test tubes and dried completely under a stream of nitrogen. The dried residues were reconstituted with 35% ACN: 65% water prior to analysis.

The extraction efficiency was determined by analyzing duplicate aliquots (15 µL) for radioactivity concentrations by LSC. For metabolite profiling, aliquots of the supernatants were injected onto the HPLC with UV and radioactivity detection. For metabolite identification, supernatants of the extracts were analyzed by HPLC/MS/MS method and also co-eluted with the metabolite standards.

Analytical Method.

Metabolite profiling and identification in plasma, urine, and feces was performed on a high-performance liquid chromatography (HPLC) column coupled to radioactive, ultraviolet (UV) and mass spectrometry (MS) detectors. The integrated system consisted of Agilent 1100 HPLC with quaternary pumps, autosampler, diode array UV detector, LTQ-Orbitrap mass spectrometer (Thermo Scientific, San Jose, CA) and a Perkin Elmer 625TR radioactivity flow detector. The radioactivity flow detector, Flow-one, equipped with a 100 µL flow cell, was operated using scintillation cocktail (Ultima Flo M) at flow rate of 1.5 mL/min. Chromatography was accomplished on a Phenomenex Luna, C18 (2) column (4.6 × 250 mm, 5 µm

[Torrance, CA, USA]). The column was kept at ambient temperature during the analysis of samples. Mobile phase A was 40 mM of ammonium formate (NH_4FA), pH 3.2, in water, and mobile phase B was ACN. The details of the mobile phase gradient used can be found in the supplemental material (Supplemental Table 2). The first 5 min of the HPLC flow was diverted to the waste prior to evaluation of metabolites. The UV absorption spectra from 200–400 nm was recorded using the diode array UV detector. A ThermoFinnigan LTQ-Orbitrap mass spectrometer (Thermo Scientific, San Jose, CA, USA) equipped with an electrospray ionization (ESI) interface operated in positive ionization mode for metabolite profiling and identification. Mass spectra were acquired in full scan (MS) *(m/z* 200–1000) and data dependent scan (MS2, MS3, and MS4) modes.

Data Analysis and Calculations

Xcalibur (version 2.07) was used to acquire mass spectral data and UV absorption data on LTQ LC/MS systems, respectively. It was also used to control the various components of the LC/UV/MS system and was utilized to process the data. Laura (version 3.3) was used to control β-RAM and acquire radiochromatograms. TopCount NXT™ was operated by Windows NT®-based Hologram® relational database software. Analyst (version 1.4.1) was used to control the LC/MS analysis performed on Shimadzu-API4000 system (acquisition and processing of the data).

Identification and Characterization of Metabolites

The structures of the metabolites were identified by LC/MS/MS based on comparison of mass spectral fragmentation patterns with those produced by the

parent compound under the same experimental conditions. The proposed structures were also confirmed with the elemental composition based on the accurate mass values obtained on Orbitrap mass spectrometer. The structures of metabolites were also confirmed by comparison with synthetic reference standards. The comparisons included determining the accurate molecular weights, HPLC retention times and fragmentation patterns of the observed metabolites and reference standards. The chlorine isotopic distribution pattern (ratio of 3:1) was also used as a diagnostic tool for metabolite confirmation. The high-resolution mass spectra of alisertib and its metabolites can be found in the supplemental material (Supplemental Figure 1 through Supplemental Figure15). Product ion scans for metabolite M10 could not be obtained due to weak signal.

Determination of Alisertib, M1, and M2 Concentrations in Pooled Plasma by LC/MS/MS

Concentrations of alisertib and its metabolites M1 and M2 were obtained from the pooled plasma samples using a verified LC/MS/MS method. Details of the procedures used to quantitate alisertib and its metabolites in pooled human plasma are provided below. Several analyses were conducted to determine the concentrations of these compounds in plasma samples. Additional verification of LC/MS/MS method was performed so that reliable estimates of alisertib and its metabolites could be obtained in plasma samples.

Stock Solution Preparation

Primary stock solution (PSS):

Alisertib: 2.3 mg of alisertib sodium (active moiety 95.93%) was dissolved into 2.2 mL of 1: 1 acetonitrile (ACN): DMSO, v/v) to obtain a 1 mg/mL solution.

M1: 1.5 mg of M1 powder was dissolved into 1.5 mL of 1: 1 acetonitrile (ACN): DMSO, v/v) to obtain a 1 mg/mL solution.

M2: 1.2 mg of M2 powder was dissolved into 1.2 mL of 1: 1 acetonitrile (ACN): DMSO, v/v) to obtain a 1 mg/mL solution.

Secondary stock solution (SSS): 3-in-1 containing alisertib, M1 and M2: Aliquots of 20 µL of PSS of alisertib, M1 and M2 were added in a polypropylene tube/vial and volume made up to 1 mL with ACN to prepare a 3-in-1 SSS (alisertib, M1 and M2).

Standard Curve and Quality Control (QC) Preparation: Highest calibrator (STD 9, 1000 ng/mL of alisertib, M1 and M2): An aliquot (0.05 mL) of SSS (20 µg/mL of alisertib, M1 and M2) was diluted to 1 mL with blank human plasma.

Calibration curve: serial dilution was performed with blank human plasma to prepare the calibrators at 1000, 900, 500, 200, 100, 50, 20, 10, 5 and 1 ng/mL of 3-in-1 (alisertib, M1 and M2).

Four QC Samples: The 3-in-1 (alisertib, M1 and M2) QC samples were prepared at 5, 15, 150, and 750 ng/mL. Further details of QC sample preparation can be found in the supplemental material (Supplemental Table 3). Higher concentration standards or QC samples in blank human plasma, and stored at -70°C for minimum of 12 hours prior to use or extraction.

Sample Extractions

Aliquots (0.05 mL) of control human plasma, clinical plasma samples, calibrators, and QC samples were placed in individual wells of a 1 mL 96-well (Costar round bottom) plate. To each well (excluding blank) an aliquot (0.2 mL) of

acetonitrile with internal standard working solution ($^{13}C,D_3,^{15}N_2$-alisertib at 200 ng/mL) was added and vortexed gently, followed by centrifugation for approximately 10 min. A portion (0.1 mL) of supernatant was transferred to an injection vial plate containing 0.15 mL of water followed by vortexing. Following centrifugation at 3500 rpm for 10 min, aliquots (5 μL) of sample were injected onto an API 4000 LC/MS/MS system.

Quantitative Analysis by LC/MS/MS

The human plasma extracts were analyzed using a LC/MS/MS system consisting of Shimadzu LC-10AD Pumps SIL-HTc autosampler interfaced to an API 4000 triple quadruple mass spectrometer equipped with an electrospray ionization (ESI) source. Chromatographic separations were achieved utilizing an ACE3 C8, 50 x 4.6 mm, 5μ (ACT, UK) column. Details of the LC gradient used can be found in the supplemental material (Supplemental Table 4). The first 1.5 minutes of the HPLC flow was diverted to waste.

The API 4000 mass spectrometer was equipped with an electrospray ionization (ESI) interface and operated in the positive ion mode. The mass spectrometer was operated in Multiple Reaction Monitoring (MRM) mode. The details of the mass spectrometer settings and transitions utilized for quantitative analysis can be found in the supplemental material (Supplemental Table 5).

Cytochrome P450 Phenotyping Assay

Human complementary deoxyribonucleic acid (cDNA)-expressed recombinant cytochrome P450 (rCYP) isozymes CYP1A2, 2B6, 2C8, 2C9, 2C19, 2D6, and 3A4 Supersomes™ (BD Biosciences, Woburn, MA, USA) and human liver microsomes (pool of 100 male and 100 female; XenoTech, LLC, Lenexa, KS, USA) were diluted

DMD Fast Forward. Published on January 7, 2020 as DOI: 10.1124/dmd.119.087338
This article has not been copyedited and formatted. The final version may differ from this version.

with phosphate buffer (0.1 M; pH 7.4) to yield a concentration of 20 pmol/mL Supersomes™ and 0.5 mg/mL human liver microsomes in the final incubation. Separately, 8 mM NADPH and 12 mM $MgCl_2$ (2 mM NADPH and 3 mM $MgCl_2$, final assay concentration) were combined with an equal volume of 40 µM alisertib (10 µM final concentration). A sample of 150 µL of the NADPH/$MgCl_2$/alisertib mixture was then aliquotted into a 96-well plate. The plate containing the150 µL of the NADPH/$MgCl_2$/alisertib mixture, and the individual Supersomes and human liver microsomes were then warmed at 37ºC for 4 min. The reaction was initiated by the addition of an equal volume (150 µL) of Supersomes™ or human liver microsomes into the plate containing the NADPH/ $MgCl_2$/alisertib mixture. Reactions were terminated after 0 or 15 minutes by aliquotting 0.1 mL of incubate into 0.1 mL of cold acetonitrile containing 0.5 µM carbutamide (internal standard). Precipitated protein was removed by centrifugation (1800 × g for 10 min at 0ºC), and the supernatant was analyzed by liquid chromatography with tandem mass spectrometry (LC/MS/MS).

Standard curves (0 to 3 µM) were used to quantitate the metabolite peaks in the samples generated with human liver microsomes or rCYPs. Curves with total metabolite (M2 and M3) concentrations of 0, 0.0029, 0.0059, 0.0117, 0.0234, 0.0469, 0.0938, 0.1875, 0.375, 0.75, 1.5, and 3 µM were set up by adding equal volumes of solution containing M2 and M3, each at 12 µM, and performing 10 further serial dilutions at a ratio of 1:1 sample to diluent. Then, an equal amount of Supersomes™ control protein or human liver microsomes and alisertib (0.25 mg/mL and 2.5 µM final concentration, respectively) combined, was added to the metabolite dilutions to further dilute their concentration by a factor of 2.

DMD Fast Forward. Published on January 7, 2020 as DOI: 10.1124/dmd.119.087338
This article has not been copyedited and formatted. The final version may differ from this version.

The contribution of each individual human CYP isozyme (from the Supersomes™) towards the overall rate of metabolism determined in human liver microsomes was calculated according to the equation 1:

Equation 1:

Y = [(Rate of Individual CYP Isozyme Metabolism × RAF)/(Rate of Metabolism in human liver microsomes)] × 100

Where, RAF = relative activity factor as determined for individual CYP and is equal to the ratio of intrinsic clearance (CL_{int}) of CYP selective probe substrate clearance in rCYP to that in human liver microsomes (HLM) (Equation 2).

Equation 2:

$RAF = CL_{int,CYP\ rCYP}/CL_{int,CYP,HLM}$

For detection of alisertib and its metabolites (M2 and M3), aliquots of the supernatants were injected onto an LC/MS/MS system consisting of an Agilent 1290 ultra high-performance liquid chromatography (UHPLC) system (Agilent Technologies, Palo Alto, CA, USA) coupled to a Synergi Hydro-RP C18 column (2.5 µm; 50 × 3.0 mm) (Phenomenex, Inc., Torrance, CA, USA) at 35°C. Solvent A was 0.1% formic acid in HPLC-grade water and Solvent B was 0.1% formic acid in HPLC-grade acetonitrile. The LC gradient conditions for the method can be found in the supplemental material (Supplementary Table 6).

The UHPLC eluent was introduced via electrospray positive ionization directly into an AB SCIEX API 6500 QTRAP triple quadrupole linear ion trap mass spectrometer (AB SCIEX, Framingham, MA, USA). The sample injection volume was 3 µL. Alisertib and metabolites M2 and M3, and the internal standard, were detected

by electrospray ionization with tandem mass spectrometry (ESI-MS/MS) in positive ion mode. The parameter settings for the AB SCIEX API 6500 QTRAP mass spectrometer can be found in the supplemental material (Supplemental Table 7).

Standard curves and quantitation of the peak areas of the metabolites were performed using Analyst software, Version 1.6 (AB SCIEX). CYP isozyme contributions were determined by dividing the mean peak area of either metabolite by the sum of the mean peak area of all the metabolites.

UGT Phenotyping Assay

The ^{14}C-Alisertib stock solution was prepared in 0.1-M potassium phosphate buffer (pH 7.4) with 1% ACN. In a 96-well plate, human complementary deoxyribonucleic acid (cDNA)-expressed UGT supersomes (1.0-mg/mL final concentration) with alamethicin (50 µg/mg microsomal protein) were prewarmed, in duplicate, with ^{14}C-Alisertib (10-µM final concentration) for 5 minutes at 37°C. The reactions were initiated by the addition of UDPGA (2.5-mM final concentrations) with $MgCl_2$ (3-mM final concentration) and incubated for 0 or 30 minutes. The total volume in each well was 250 µL. The reactions were terminated by the addition of equal volumes of ACN. The sample plates were centrifuged at 1800 × g for 10 minutes and the supernatants were analyzed using reverse-phase HPLC with an in-line β-RAM radiochemical detector.

The HPLC system consisted of an Agilent 1100 binary pump (Agilent Technologies, Palo Alto, CA, USA) coupled to an IN/US β-RAM detector (IN/US Systems, Inc., Tampa, FL, USA). Alisertib and its metabolites were resolved at a 0.7-mL/min flow rate using a Luna C18(2) column (4.6 × 150 mm, 3 µm) (Phenomenex, Inc., Torrance, CA, USA). The peak areas of Alisertib and its metabolites were

determined using an in-line β-RAM detector with 1:2 (volume-to-volume ratio [v:v]) infusion of In-Flow 2:1 liquid scintillator (IN/US Systems, Inc., Tampa, FL, USA) and integrated with LauraLite software (Version 3.2.4.17; LabLogic Systems, LTC, Sheffield, England). The sample injection volume was 100 µL. Mobile phases A and B were water and ACN, respectively, each supplemented with 0.1% v:v formic acid. The LC gradient details can be found in the supplemental material (Supplementary Table 8).

CYP Inhibition

Human liver microsomes (pool of 100 male and 100 female; 0.2 mg/mL in 0.1 M potassium phosphate buffer, pH 7.4; XenoTech, LLC, Lenexa, KS, USA) were incubated in 96-well plates with CYP isozyme-selective substrates and multiple concentrations of alisertib (0 to 100-µM), M1 (0 to 100 µM), or M2 (0 to 50 µM). The CYP isozyme-selective substrates that were used included phenacetin (CYP1A2; 30 µM final concentration; metabolite, acetaminophen), bupropion (CYP2B6; 100 µM; metabolite, hydroxybupropion), amodiaquine (CYP2C8; 1 µM; metabolite, desethylamodiaquine), diclofenac (CYP2C9; 15 µM; metabolite, hydroxydiclofenac), (*S*)-mephenytoin (CYP2C19; 100 µM; metabolite, hydroxy[*S*]-mephenytoin), dextromethorphan (CYP2D6; 5 µM; metabolite, dextrorphan), midazolam (CYP3A4/5; 5 µM; metabolite, 1'-hydroxymidazolam), and testosterone (CYP3A4/5; 5 µM; metabolite, 6β-hydroxytestosterone). Corresponding CYP inhibitors used in the assay were furafylline (CYP1A2; 20 µM final concentration), ticlopidine (CYP2B6; 20 µM), quercetin (CYP2C8; 25 µM), sulfaphenazole (CYP2C9; 20 µM), ticlopidine (CYP2C19; 20 µM), quinidine (CYP2D6; 10 µM), and ketoconazole (CYP3A; 10 µM).

Reactions were initiated by adding NADPH (2 mM) and $MgCl_2$ (3 mM) to the preincubated human liver microsome mix, for a total volume of 100 µL. Reactions were incubated for 12 min at 37°C, except for CYP2C8, which was incubated for 8 min. The reactions were then terminated by adding an equal volume of acetonitrile containing 0.5 µM carbutamide (internal standard). After termination with acetonitrile, the plates were centrifuged at 1800 × g for 10 min at 0°C to pellet the precipitated proteins. The supernatants were analyzed by liquid chromatography with tandem mass spectrometry (LC/MS/MS) to determine the amount of metabolite formed by each CYP isozyme.

Analytes were separated on a Phenomenex Synergi Hydro-RP C18 column (50 × 3.0 mm, 2.5 µm particle size) (Phenomenex, Inc., Torrance, CA, USA) using a gradient comprising 0.1% formic acid in water (Solvent A) and 0.1% formic acid in acetonitrile (Solvent B) at a flow rate of 0.9 mL/min. All analytes were detected by positive ion spray in Multiple Reaction Monitoring (MRM) mode using an API 4000 or 6500 LC/MS/MS system (Applied Biosystems, Inc., Carlsbad, CA, USA).

The peak area ratio of each analyte to the internal standard (i.e. the peak area of acetaminophen, hydroxybupropion, desethylamodiaquine, hydroxydiclofenac, hydroxy(*S*)-mephenytoin, dextrorphan, 1′-hydroxymidazolam, or 6β-hydroxytestosterone formed over the peak area of carbutamide) was quantified using Analyst software, Version 1.6 (AB SCIEX, Foster City, CA, USA). The percentage inhibition of CYP isozyme activity was calculated for each concentration of alisertib, M1, and M2, and the percentages were plotted against the concentrations of alisertib/M1/M2 using XLFit (ID Business Solutions Ltd, Cambridge, MA, USA). The sigmoidal dose-response (variable slope) model was used to determine IC_{50} values, which were rounded to the nearest whole number, according to the following

calculation, where X is the logarithm of concentration, and Y is the percent activity (Equation 3):

Equation 3:

$$Y = \text{Minimum activity} + (\text{Maximum activity} - \text{Minimum activity}) / (1 + 10[\text{Log}^{(IC50-X) * \text{HillSlope}]})$$

DMD Fast Forward. Published on January 7, 2020 as DOI: 10.1124/dmd.119.087338
This article has not been copyedited and formatted. The final version may differ from this version.

Results

Patients. There were no clinically relevant findings with regards to medical history, previous medication, serology, or physical examination at screening of the patients. All three patients had received prior therapy and undergone prior surgery for their solid tumors, with two patients (with bladder cancer and mesothelioma, respectively) receiving prior radiation therapy.

Metabolic Profiling. The total recovery of administered radioactivity (mass balance), routes of excretion, and pharmacokinetics of [^{14}C]-alisertib were presented separately (Zhou et al 2018a). Briefly, following a single 35 mg dose of [^{14}C]-alisertib oral solution containing ~80 µCi of TRA, a mean of 90.5% of the total administered radioactivity was recovered in excreta (urine and feces combined) by 14 days post-dose. In general, a mass balance recovery of 80% and higher is considered acceptable in human ADME studies (Roffey et al. 2007). The majority (mean 87.8%) of the radioactivity was cleared via the fecal route; renal excretion was a minor route of clearance (mean 2.7%). The mean percentage cumulative recovery of total radioactivity in urine and feces and combined recovery in excreta is presented in Figure 1 (reproduced from Zhou et al, 2018a). The mean concentration-time profiles of alisertib and total radioactivity in plasma are shown in Figure 2 (reproduced from Zhou et al, 2018a). Based upon the plasma AUC_{inf} for alisertib and total radioactivity, 45% of the plasma radioactivity is associated with alisertib (Zhou et al, 2018a).

Table 1 summarizes the metabolites of [^{14}C]-alisertib observed in 0–192 hour plasma, urine, and fecal samples, and the identities of proposed metabolites, accurate mass (protonated ion, $[M+H]^+$, mass-to-charge [*m/z*]) values (both

measured and calculated), and HPLC retention times of each metabolite. The high-resolution mass spectra (product ion scans) of alisertib and its metabolites are presented in Supplemental Figure 1 through Supplemental Figure 15.

Plasma. The mean plasma extraction recovery post reconstitution was >75% across the three patients. Some of the loss in recovery was estimated to be due to the complete drying of sample and incomplete recovery post reconstitution. The column recovery of radioactivity was evaluated during method development was deemed to be quantitative.

The pooling of plasma over 0- to 192-hour post-dose was intended to approximate the steady-state concentration of alisertib and its metabolites, as >90% (> 4 x terminal half-life [$t_{1/2}$] of TRA elimination) of circulating drug-related radioactivity was eliminated from plasma by 192-hours post-dose (Zhou et al.). Individual patient radiochromatograms showing the metabolite profiles of [^{14}C]-alisertib from pooled plasma samples collected between 0–192 hours post-dose are shown in Figure 3. The estimated metabolite peak area, concentration, $AUC_{0–192\ hour}$, and metabolite percentage relative to alisertib for each patient, based on the analyte peak area in the radiochromatograms are listed in Table 2. Alisertib and *O*-desmethyl alisertib (M2) were the major drug-related components in the pooled 0–192 hour plasma samples from all three patients. M1 (consisting of two isomers M1a and M1b, Table 2) and M3 were minor components observed in plasma. The acyl glucuronide M1 in plasma was found to isomerize to two peaks during the drying of plasma extract and reconstitution. Plasma extract when injected directly on the mass spectrometer without any drying process showed only a single peak for the acyl glucuronide conjugate, M1. Furthermore, in a prior study, acyl glucuronide was

shown to be stable in plasma. The [^{14}C]-labeled acyl glucuronide was spiked into pre-dose plasma (acidified and non-acidified) followed by incubations at 37°C for up to 2 hours. There was no decrease in the [^{14}C]-acyl glucuronide peak area nor was there formation of the aglycone, alisertib, or any other peaks from acyl migration detected under either condition (unpublished data). Hence, the two peaks seen in the plasma profile were combined to represent the acyl glucuronide conjugate concentration. The mean relative percentages of M1, M2, and M3 were 23%, 74%, and 12% compared with alisertib. The mean relative percentages of alisertib, M1, M2, and M3 in plasma were 48%, 12%, 35%, and 6% of the total plasma radioactivity, respectively.

Quantitative determination of alisertib and its metabolites, M1 and M2, in 0-192 hour pooled plasma by LC/MS/MS also provided similar results to the ones determined using radioactivity profiles. The average concentrations of alisertib, M1, and M2 by LC/MS/MS were 76.3, 15.9, and 40.9 ng/mL, respectively, whereas that determined by radioactivity profiles were 49.7, 12.6, and 36.0 ng/mL, respectively. The slightly lower recovery in the radiolabeled profiles could potentially be explained by lower extraction recovery.

Urine. The extraction recovery of total radioactivity in urine was deemed to be quantitative. Individual patient radiochromatograms showing the metabolite profiles of [^{14}C]-alisertib from pooled urine samples collected between 0–192 hours post-dose are shown in Figure 4. Unchanged [^{14}C]-alisertib was a minor drug-related component in urine and was detected only by the LC/MS method. Four glucuronide conjugates and one metabolite resulting from hydroxylation and hydrogenation were observed in the pooled 0–192 hour urine samples from each patient. These included

the acyl glucuronide conjugate of alisertib (M1), glucuronide conjugates of *O*-desmethyl alisertib (M7 and M8), glucuronide conjugate of hydroxy alisertib (M9), and a hydroxylated/hydrogenated analogue of alisertib (M6). The estimated percentage of dose of each observed metabolite in urine is listed in Table 3. Due to the mean urine excretion being < 3% of the total administered radioactivity, the estimated percentages of the dose of each metabolite in urine samples were all very low and less than 2% of the dose (Table 3). In prior studies, the acyl glucuronide, M1, was shown to be stable in urine. The [^{14}C]-labeled acyl glucuronide was spiked into pre-dose urine (acidified and non-acidified) followed by incubations at 37°C for up to 2 hours. There was no decrease in the [^{14}C]-acyl glucuronide peak area nor was there formation of the aglycone, alisertib, or any other peaks from acyl migration detected under either conditions (unpublished data).

Feces. The mean fecal extraction recovery was >70% across the three patients. Individual patient radiochromatograms demonstrating the metabolite profiles of [^{14}C]-alisertib from pooled fecal extracts collected between 0–192 hours post-dose are shown in Figure 5. A total of 11 metabolites derived from *O*-demethylation, hydroxylation, oxidative deamination, hydroxylation/hydrogenation, or combinations of various metabolic reactions were detected in fecal samples. These included M2, hydroxy alisertib (M3, M4, M5), *O*-desmethyl-hydroxy- alisertib (M10, M11, and M12), oxidative deaminated alisertib (M14 and M15), hydroxylated/hydrogenated alisertib (M6), and dihydroxy alisertib (M13). The estimated percentages of the dose of each metabolite observed in feces, based upon the metabolite peak area, are listed in Table 3. Among these, M3 was one of the major drug-related components excreted in feces along with unchanged [^{14}C]-

alisertib. Unchanged alisertib was one of the major drug-related components in the 0–192 hour pooled fecal extracts, accounting for 12–40% (mean 26%) of the dose administered. Metabolite M3 accounted for 19–22% (mean 21%) of the dose administered. The rest of the metabolites were all less than 10% of the dose administered (Table 3).

Metabolites M2 and hydroxy alisertib (M3, M4, and M5) were the primary phase I oxidative metabolites detected in feces, with all other metabolites resulting from further metabolism of these four primary metabolites. The majority of the metabolites identified in feces were the result of further metabolism of M2 and M3. Of the 83.4% of the dose excreted in feces over 0–192 hours post-dose, phase I oxidative metabolites accounted for 57.1% of the dose, the rest being unchanged alisertib (Table 4). Extrapolating the 86.2% of the dose excreted in urine and feces combined to 100% recovery, it can be inferred that 68% of the total radioactivity in excreta was accounted for by metabolites derived from phase I oxidative metabolism (Table 4).

Drug-Drug Interaction Potential of Alisertib and its Metabolites. CYP reaction phenotyping, as determined by evaluation in human cDNA-expressed rCYP isozymes with relative activity factors (RAFs), showed that the relative percentage contributions of CYP isozymes to the formation of M2 and M3 followed the order: CYP3A4 (86%) > CYP2C8 (7%) > CYP2C9 (4%) > CYP1A2 (2%) > CYP2C19, 2B6, and 2D6 (all <1%) (Table 5).

The UGT phenotyping experiment had indicated that UGT1A1, UGT1A3, and UGT1A8 were the major isozymes responsible for acyl glucuronidation of alisertib with 11%, 10%, and 79% relative enzyme activity, respectively, towards alisertib

glucuronidation without correction for abundance of UGT isozymes (Table 6). The alisertib acyl glucuronide formation was not detected with the other UGT isozymes tested.

In the in-vitro drug-drug interaction studies, the alisertib metabolites M1 and M2 showed no appreciable reversible inhibition of CYP1A2, 2B6, 2C8, 2C9, 2C19, 2D6, and 3A4/5 activities with IC50 values greater than 100 μM and 50 μM for M1 and M2, respectively, the maximum concentrations tested (Table 7).

DMD Fast Forward. Published on January 7, 2020 as DOI: 10.1124/dmd.119.087338
This article has not been copyedited and formatted. The final version may differ from this version.

Discussion

This study represents the first characterization of the biotransformation of the investigational AAK inhibitor, alisertib, in humans. The metabolic profile of alisertib was determined in plasma, urine, and fecal samples from three patients with advanced solid tumors who received a single 35 mg dose of [^{14}C]-alisertib oral solution. The 35-mg oral solution dose was expected to result in a systemic exposure (AUC) similar to that observed following administration of the ECT at the 50-mg dose used in the clinical regimen based on a previously conducted relative bioavailability study in cancer patients (Falchook et al. 2015). Results from the mass balance analysis portion of this study indicated that alisertib is predominantly cleared via the fecal route (approximately 88% of the total dose), suggesting hepatic metabolism, biliary excretion, and potentially incomplete absorption. Renal excretion accounted for less than 3% of total clearance.

Unchanged [^{14}C]-alisertib was the predominant drug-related component in circulation following a single dose of [^{14}C]-alisertib oral solution, followed by M2; M1 and M3 were minor metabolites in plasma. Only metabolites M1 and M2 were greater than 10% of the circulating radioactivity. In urine, unchanged [^{14}C]-alisertib was only a minor drug-related component, with M1 and the glucuronide conjugate of hydroxy alisertib (M9) being the major drug-related components. The estimated percentages of dose of each metabolite in urine samples were all very low and less than 2% of the total dose administered. While several metabolites derived from *O*-demethylation, hydroxylation, oxidative deamination, hydroxylation/hydrogenation, and combinations of various metabolic reactions were detected in feces, M3 was one of the major drug-related components along with the unchanged [^{14}C]-alisertib. The

unchanged alisertib could be from incomplete absorption, from hydrolysis of alisertib glucuronide by gut microflora, or biliary clearance. The majority of the other metabolites identified in feces were the result of further metabolism of the two primary phase I oxidative metabolites M2 and M3. These findings indicate that alisertib is metabolized through a combination of phase I oxidative and phase II glucuronidation pathways, primarily via *O*-demethylation of the fluoromethoxyphenyl moiety (M2), direct acyl glucuronidation (M1), and hydroxylation of the benzazepine moiety (M3). Figure 6 summarizes the proposed metabolic pathways of alisertib in humans. Overall, metabolites resulting from phase I oxidative pathways contributed to more than 58% of the dose recovered in urine and feces between 0–192 hours post-dose, which corresponds to approximately 68% of the dose when normalized for complete recovery of radioactivity in urine and feces.

The UGT phenotyping experiment had indicated that UGT1A1, UGT1A3, and UGT1A8 were the major isozymes responsible for acyl glucuronidation of alisertib with 11%, 10%, and 79% relative enzyme activity, respectively, towards alisertib glucuronidation (Table 6). However, the overall *in vitro* contribution of CYPs vs. UGTs could not be assessed with full confidence due to low *in vitro* turnover of alisertib in liver microsomes and hepatocytes in addition to the involvement of extrahepatic UGT1A8 in alisertib metabolism, which showed the highest activity.

In contrast, the *in vivo* urine and fecal metabolite profiles indicated that phase I oxidative metabolism pathways were involved in more than 68% of alisertib metabolism, primarily via M2, M3, and their downstream metabolite formation. Given the role of oxidative pathways in the metabolism of alisertib, *in vitro* CYP reaction phenotyping studies were undertaken to elucidate the CYPs involved in formation of metabolites M2 and M3.

DMD Fast Forward. Published on January 7, 2020 as DOI: 10.1124/dmd.119.087338
This article has not been copyedited and formatted. The final version may differ from this version.

Based on CYP reaction phenotyping studies, CYP3A4, with 86% contribution, was the major enzyme involved in oxidative metabolism of alisertib to M2 and M3 (Table 5). Thus, taking into account the percent contribution of oxidative metabolism (68% after normalizing for 100% recovery; Table 4) estimated in the absorption, distribution, metabolism, and excretion study and the percent contribution of CYP3A (86%) to oxidative metabolic pathways determined in the in-vitro metabolism studies, it can be inferred that CYP3A contributes to 58% of the overall apparent oral clearance of alisertib in humans. The identification of an important role of CYP3A4 in the metabolism of alisertib prompted the initiation of in-vivo drug-drug interaction studies of alisertib with the strong CYP3A inhibitor itraconazole and the strong CYP3A inducer rifampin (Zhou et al. 2018b). The strong CYP3A inhibitor itraconazole produced an approximately 40% increase in total alisertib systemic exposure (AUC) suggesting an approximately 30% contribution of CYP3A-mediated metabolism to the overall apparent clearance of orally administered alisertib. These results suggest a somewhat lower in vivo contribution of CYP3A to the overall apparent oral clearance of alisertib than would be predicted from the estimated 58% contribution of CYP3A from this ADME study and reaction phenotyping. Nevertheless, the findings are qualitatively consistent with our identification of a parallel route of direct glucuronidation that results in only a partial contribution of CYP3A-mediated metabolism to the overall clearance of alisertib in humans. As expected, co-administration of the strong CYP3A inducer rifampin produced an approximately 50% decrease in alisertib AUC and a corresponding shortening of half-life, consistent with induction of systemic metabolic clearance. Additionally, the confirmation of a major role for metabolism as the primary clearance mechanism for alisertib led to the design of a study which investigated the effect of varying degrees

of hepatic impairment on alisertib pharmacokinetics in cancer patients (NCT02214147) in order to inform appropriate dosing recommendations for these special patient populations. Moderate or severe hepatic impairment resulted in an approximately 150% increase in alisertib AUC, consistent with a major role for hepatic metabolism in the overall clearance of orally administered alisertib and indicating the need for initiating alisertib treatment at appropriately reduced starting doses in these patient populations (Zhou et al. 2016). In contrast, the results of population PK analyses indicate the lack of effect of mild hepatic impairment indicating that dose modifications of alisertib are not required in these patients (Zhou et al. 2016). As fecal excretion is the major route of clearance, the overall contribution of the direct glucuronidation pathway towards clearance of alisertib cannot be estimated with the current data. Any acyl glucuronide excreted in the gut via biliary excretion pathways will undergo hydrolysis to the aglycone, alisertib, and also become available for enterohepatic recycling. Accordingly, it is possible that the parent drug excreted in the feces could have resulted from gut microbial deconjugation of the glucuronide, biliary clearance of alisertib and/or represent unabsorbed alisertib – the relative contributions of which cannot be estimated based on the available data. UGT1A8, one of the primary isozymes responsible for alisertib acyl glucuronidation, is expressed predominantly in the gut, and any contribution of UGT1A8 to alisertib clearance via intestinal metabolism also cannot be estimated with the current data. Although UGT1A1 is one of the UGT isoforms that was identified as being able to glucuronidate alisertib in vitro, the apparent clearance of alisertib is not decreased in patients harboring the *UGT1A1*28* allele (associated with reduced enzyme expression) based on the results of population PK analyses

(Zhou et al. 2018c; Venkatakrishnan et al. 2014), suggesting only a minor in vivo contribution of UGT1A1 to overall alisertib clearance in humans.

As the two major circulating metabolites (M1 and M2) are present at 23% and 74% of the plasma alisertib levels, *in vitro* studies were conducted to further evaluate their DDI potential. Based on the in-vitro inhibition studies of M1 and M2 with a panel of CYPs, there appears to be minimal potential, at the therapeutic dose of alisertib, for M1 and M2 perpetrating clinically relevant DDI with co-administered drugs (Table 6).

The pharmacological activity of alisertib acyl glucuronide has not been determined. Although metabolite M2 is pharmacologically active, it is 4-fold less potent than alisertib in both enzyme and cell-based potency assays and also has lower plasma free fraction (0.5% free vs. 1.5% free for alisertib), and thus not expected to contribute significantly to efficacy.

The acyl glucuronide of alisertib, M1, was shown to be stable at pH 7.4 at 37°C with a half-life of 69 hours. The long half-life of the acyl glucuronide, M1, in buffer indicates that the potential for acyl migration is very low (Sawamura et al., 2010; Vanderhoeven et al., 2004; Iwamura et al., 2017; Van Vleet et al., 2017). In addition, prior studies had also indicated that the acyl glucuronide of alisertib was stable in acidified or non-acidified plasma and urine following incubations at 37°C for up to 2 hours under both conditions. All metabolites identified in this study were also identified in one or both preclinical toxicology species, rats and dogs. The major circulating metabolites of alisertib showed adequate coverage in rats (Table 8; unpublished data).

This study is limited by the small numbers of patients included; although it is reassuring that our findings were generally consistent across all three patients.

Nevertheless, the results of this metabolic profiling analysis in humans are consistent with data from preclinical studies in rats showing that alisertib is metabolized through both glucuronidation and oxidative pathways (Millennium Pharmaceuticals, Inc., unpublished data). Importantly, the results of this study and follow-on CYP reaction phenotyping studies have pointed to CYP3A4 being a principal enzyme that mediates the oxidative metabolism of alisertib, resulting in the design of clinical DDI studies with the strong CYP3A inhibitor itraconazole and the strong CYP3A inducer rifampin, where alisertib exposures were increased by approximately 40% and decreased by approximately 50%, respectively. Viewed in broader context, this example illustrates the value of timely conduct of human ADME studies in providing guidance to the clinical pharmacology development program for oncology drugs, for which a careful understanding of sources of exposure variability is crucial to inform risk management for DDIs given the generally limited therapeutic window for anticancer drugs and polypharmacy that is common in cancer patients.

Acknowledgments

The authors would like to thank all the study participants and their families. The authors thank Saeho Chong of Millennium Pharmaceuticals, Inc. for contributions to the oversight of operational aspects of this study and data analysis. We acknowledge Dawn L. Lee of FireKite, an Ashfield company, part of UDG Healthcare plc, for writing support during the development of this manuscript, which was funded by Millennium Pharmaceuticals, Inc., and complied with Good Publication Practice 3 ethical guidelines (Battisti et al., *Ann Intern Med* 2015;163:461-4). The authors would also like to thank Charles River Laboratories and Frontage Labs for the analytical support.

Author contributions

Participated in research design: Pusalkar, Zhou, Li, Cohen, Yang, Balani, Xia, Shyu, Lu, Venkatakrishnan, Chowdhury

Conducted experiments: Pusalkar, Zhou, Li, Lu, Cohen

Contributed new reagents or analytic tools: Balani

Performed data analysis: Pusalkar, Zhou, Li, Lu, Cohen, Balani

Wrote or contributed to the writing of the manuscript: ALL Authors – Pusalkar, Zhou, Li, Cohen, Yang, Balani, Xia, Shyu, Lu, Venkatakrishnan, Chowdhury

References

Bischoff JR, Anderson L, Zhu Y, Mossie K, Ng L, Souza B, Schryver B, Flanagan P, Clairvoyant F, Ginther C, Chan CS, Novotny M, Slamon DJ, and Plowman GD (1998) A homologue of Drosophila aurora kinase is oncogenic and amplified in human colorectal cancers. *EMBO J* **17:**3052-3065.

Cervantes A, Elez E, Roda D, Ecsedy J, Macarulla T, Venkatakrishnan K, Rosello S, Andreu J, Jung J, Sanchis-Garcia JM, Piera A, Blasco I, Manos L, Perez-Fidalgo JA, Fingert H, Baselga J, and Tabernero J (2012) Phase I pharmacokinetic/pharmacodynamic study of MLN8237, an investigational, oral, selective aurora a kinase inhibitor, in patients with advanced solid tumors. *Clin Cancer Res* **18:**4764-4774.

Dar AA, Goff LW, Majid S, Berlin J, and El-Rifai W (2010) Aurora kinase inhibitors--rising stars in cancer therapeutics? *Mol Cancer Ther* **9:**268-278.

Dees EC, Cohen RB, von MM, Stinchcombe TE, Liu H, Venkatakrishnan K, Manfredi M, Fingert H, Burris HA, III, and Infante JR (2012) Phase I study of aurora A kinase inhibitor MLN8237 in advanced solid tumors: safety, pharmacokinetics, pharmacodynamics, and bioavailability of two oral formulations. *Clin Cancer Res* **18:**4775-4784.

Falchook G, Kurzrock R, Gouw L, Hong D, McGregor KA, Zhou X, Shi H, Fingert H, and Sharma S (2014) Investigational Aurora A kinase inhibitor alisertib (MLN8237) as an enteric-coated tablet formulation in non-hematologic malignancies: phase 1 dose-escalation study. *Invest New Drugs* **32:**1181-1187.

Falchook GS, Venkatakrishnan K, Sarantopoulos J, Kurzrock R, Mita A, Fu S et al. (2015) Relative bioavailability of a prototype oral solution of the Aurora A kinase inhibitor

alisertib (MLN8237) in patients with advanced solid tumors. *Int J Clin Pharmacol Ther* **53**:563-572.

Friedberg JW, Mahadevan D, Cebula E, Persky D, Lossos I, Agarwal AB, Jung J, Burack R, Zhou X, Leonard EJ, Fingert H, Danaee H, and Bernstein SH (2014) Phase II study of alisertib, a selective Aurora A kinase inhibitor, in relapsed and refractory aggressive B- and T-cell non-Hodgkin lymphomas. *J Clin Oncol* **32:**44-50.

Glover DM, Leibowitz MH, McLean DA, and Parry H (1995) Mutations in aurora prevent centrosome separation leading to the formation of monopolar spindles. *Cell* **81:**95-105.

Goldberg SL, Fenaux P, Craig MD, Gyan E, Lister J, Kassis J, Pigneux A, Schiller GJ, Jung J, Jane LE, Fingert H, and Westervelt P (2014) An exploratory phase 2 study of investigational Aurora A kinase inhibitor alisertib (MLN8237) in acute myelogenous leukemia and myelodysplastic syndromes. *Leuk Res Rep* **3:**58-61.

Gritsko TM, Coppola D, Paciga JE, Yang L, Sun M, Shelley SA, Fiorica JV, Nicosia SV, and Cheng JQ (2003) Activation and overexpression of centrosome kinase BTAK/Aurora-A in human ovarian cancer. *Clin Cancer Res* **9:**1420-1426.

Hamilton RA, Garnett WR, and Kline BJ (1981) Determination of mean valproic acid serum level by assay of a single pooled sample. *Clin Pharmacol Ther* **29:**408-413.

Hirota T, Kunitoku N, Sasayama T, Marumoto T, Zhang D, Nitta M, Hatakeyama K, and Saya H (2003) Aurora-A and an interacting activator, the LIM protein Ajuba, are required for mitotic commitment in human cells. *Cell* **114:**585-598.

Hoar K, Chakravarty A, Rabino C, Wysong D, Bowman D, Roy N, and Ecsedy JA (2007) MLN8054, a small-molecule inhibitor of Aurora A, causes spindle pole and chromosome congression defects leading to aneuploidy. *Mol Cell Biol* **27:**4513-4525.

Iwamura A, Nakajima M, Oda S, Yokoi T (2017) Toxicological potential of acyl glucuronides and its assessment. *Drug Metabolsim and Pharmacokinetics* **32**:2-11.

Kaestner P, Stolz A, and Bastians H (2009) Determinants for the efficiency of anticancer drugs targeting either Aurora-A or Aurora-B kinases in human colon carcinoma cells. *Mol Cancer Ther* **8:**2046-2056.

Katayama H, Sen S (2010) Aurora kinase inhibitors as anticancer molecules. *Biochim Biophys Acta* **1799:**829-839.

Kelly KR, Shea TC, Goy A, Berdeja JG, Reeder CB, McDonagh KT, Zhou X, Danaee H, Liu H, Ecsedy JA, Niu H, Benaim E, and Iyer SP (2014) Phase I study of MLN8237--investigational Aurora A kinase inhibitor--in relapsed/refractory multiple myeloma, non-Hodgkin lymphoma and chronic lymphocytic leukemia. *Invest New Drugs* **32:**489-499.

Kitzen JJ, de Jonge MJ, and Verweij J (2010) Aurora kinase inhibitors. *Crit Rev Oncol Hematol* **73:**99-110.

Lee EC, Frolov A, Li R, Ayala G, and Greenberg NM (2006) Targeting Aurora kinases for the treatment of prostate cancer. *Cancer Res* **66:**4996-5002.

Marumoto T, Honda S, Hara T, Nitta M, Hirota T, Kohmura E, and Saya H (2003) Aurora-A kinase maintains the fidelity of early and late mitotic events in HeLa cells. *J Biol Chem* **278:**51786-51795.

Matulonis UA, Sharma S, Ghamande S, Gordon MS, Del Prete SA, Ray-Coquard I, Kutarska E, Liu H, Fingert H, Zhou X, Danaee H, and Schilder RJ (2012) Phase II study of MLN8237 (alisertib), an investigational Aurora A kinase inhibitor, in patients with platinum-resistant or -refractory epithelial ovarian, fallopian tube, or primary peritoneal carcinoma. *Gynecol Oncol* **127:**63-69.

Mazumdar A, Henderson YC, El-Naggar AK, Sen S, and Clayman GL (2009) Aurora kinase A inhibition and paclitaxel as targeted combination therapy for head and neck squamous cell carcinoma. *Head Neck* **31:**625-634.

Melichar B, Adenis A, Lockhart AC, Bennouna J, Dees EC, Kayaleh O, Obermannova R, DeMichele A, Zatloukal P, Zhang B, Ullmann CD, and Schusterbauer C (2015) Safety and activity of alisertib, an investigational aurora kinase A inhibitor, in patients with breast cancer, small-cell lung cancer, non-small-cell lung cancer, head and neck squamous-cell carcinoma, and gastro-oesophageal adenocarcinoma: a five-arm phase 2 study. *Lancet Oncol* **16:**395-405.

Park HS, Park WS, Bondaruk J, Tanaka N, Katayama H, Lee S, Spiess PE, Steinberg JR, Wang Z, Katz RL, Dinney C, Elias KJ, Lotan Y, Naeem RC, Baggerly K, Sen S, Grossman HB, and Czerniak B (2008) Quantitation of Aurora kinase A gene copy number in urine sediments and bladder cancer detection. *J Natl Cancer Inst* **100:**1401-1411.

Roffey SJ, Obach RS, Gedge JI, Smith DA (2007) What is the objective of the mass balance study? A retrospective analysis of data in animal and human excretion studies emptying radiolabeled drugs. Drug Metab Rev **39(1)**:17-43

Rojanala S, Han H, Munoz RM, Browne W, Nagle R, Von Hoff DD, and Bearss DJ (2004) The mitotic serine threonine kinase, Aurora-2, is a potential target for drug development in human pancreatic cancer. *Mol Cancer Ther* **3:**451-457.

Sasai K, Parant JM, Brandt ME, Carter J, Adams HP, Stass SA, Killary AM, Katayama H, and Sen S (2008) Targeted disruption of Aurora A causes abnormal mitotic spindle assembly, chromosome misalignment and embryonic lethality. *Oncogene* **27:**4122-4127.

Sawamaura R, Okudaira N, Watanabe K, Murai T, Kobayashi Y, Tachibana M, Ohnuki T, Masuda K, Honma H, Kurihara A, and Okazaki O (2010) Predictability of idiosyncratic drug toxicity risk for carboxylic acid-containing drugs based on the chemical stability of acyl glucuronide. *Drug Metabolism and Disposition* **38(10)**:1857-1864.

Sells TB, Chau R, Ecsedy JA, Gershman RE, Hoar K, Huck J, Janowick DA, Kadambi VJ, LeRoy PJ, Stirling M, Stroud SG, Vos TJ, Weatherhead GS, Wysong DR, Zhang M, Balani SK, Bolen JB, Manfredi MG, and Claiborne CF (2015) MLN8054 and alisertib (MLN8237): Discovery of selective oral Aurora A inhibitors. *ACS Medicinal Chemistry Letters* **6(6)**:630-634

Vanderhoeven SJ, Lindon JC, Troke J, Tranter GE, Wilson ID, and Nicholson JK (2004) NMR and QSAR studies on the transacylation reactivity of model 1b-O-acyl glucuronides. I: design, synthesis and degradation rate measurement. *Xenobiotica* **34(1)**:73-85.

Van Vleet TR, Liu H, Lee A, Blomme EAG (2017) Acyl glucuronide metabolites: implications for drug safety assessment. *Toxicology Letters* **272**:1-7.

Venkatakrishnan K, Zhou X, Ecsedy J, Mould DR, Liu H, Danaee H, Fingert H, Kleinfield R, and Milton A (2015) Dose selection for the investigational anticancer agent alisertib (MLN8237): Pharmacokinetics, pharmacodynamics, and exposure-safety relationships. *J Clin Pharmacol* **55:**336-347.

Wang X, Zhou YX, Qiao W, Tominaga Y, Ouchi M, Ouchi T, and Deng CX (2006) Overexpression of aurora kinase A in mouse mammary epithelium induces genetic instability preceding mammary tumor formation. *Oncogene* **25:**7148-7158.

Zhang XH, Rao M, Loprieato JA, Hong JA, Zhao M, Chen GZ, Humphries AE, Nguyen DM, Trepel JB, Yu X, and Schrump DS (2008) Aurora A, Aurora B and survivin are novel

targets of transcriptional regulation by histone deacetylase inhibitors in non-small cell lung cancer. *Cancer Biol Ther* **7:**1388-1397.

Zhou, X, Lockhart AC, Fu S, Nemunaitis J, Sarantopoulos J, Smith D, Muehler A, Rangachari L, Bargfrede M, Huebner D, Venkatakrishnan K (2016) Pharmacokinetics (PK) of alisertib (MLN8237) in adult patients (pts) with advanced solid tumors or relapsed/refractory lymphoma with varying degress of hepatic function. Poster presentation at 28th EORTC-NCI-AACR Symposium on Molecular Targets and Cancer Therapeutics

Zhou, X, Pusalkar, S, Chowdhury, SK, Searle S, Li Y, Ulmann CD, Venkatakrishnan V (2018a) Mass balance, routes of excretion, and pharmacokinetics of investigational oral [^{14}C]-alisertib (MLN8237), an Aurora A kinase inhibitor in patients with advanced solid tumors**.** *Invest New Drugs*. https://doi.org/10.1007/s10637-018-0693-7

Zhou, X, Pant S, Nemunaitis J, Craug Lockhart A, Falchook G, Bauer TM, Patel M, Sarantopoulos J, Bargfrede M, Muehler A, Rangachari L, Zhang B, Venkatakrishnan K. (2018b) Effects of rifampin, itraconazole and esomeparzole on the pharmacokinetics of alisertib, an investigational Aurora A kinase inhibitor in patients with advanced malignancies. *Invest New Drugs* 36(2): 248-258

Zhou, X, Mould DR, Takubo T, Sheldon-Waniga E, Heubner D, Milton A, and Venkatakrishnan K (2018c) Global population pharmacokinetics of the investigational Aurora A kinase inhibitor alisertib in cancer patients: rationale for lower dosage in asia. *Br J Clinical Pharmcol* 84: 35-51

DMD Fast Forward. Published on January 7, 2020 as DOI: 10.1124/dmd.119.087338
This article has not been copyedited and formatted. The final version may differ from this version.

Footnotes

Financial support: This study was funded by Millennium Pharmaceuticals, Inc., a wholly owned subsidiary of Takeda Pharmaceutical Company Limited.

Prior presentation: Sandeepraj Pusalkar, Xiaofei Zhou, Yuexian Li, et al. Absorption, metabolism, and excretion of alisertib (MLN8237), an Aurora A kinase inhibitor, in patients with advanced solid tumors or lymphomas. Poster presented at the 19th North American International Society for the Study of Xenobiotics (ISSX)/29th Japanese Society for the study of Xenobiotics (JSSX) Meeting; 19–23 October 2014; San Francisco, CA, USA. Abstract P331.

Current affiliation for Dr Chuang Lu:

Department of DMPK, Sanofi USA, 153 Second Avenue, Waltham, MA, 02451, USA.

Current affiliation for Dr Johnny Yang:

iHOPE Hill, LLC, Cambridge, MA, 02139, USA

Reprint requests should be addressed to:

Dr Sandeepraj Pusalkar

Drug Metabolism and Pharmacokinetics, Millennium Pharmaceuticals, Inc., a wholly owned subsidiary of Takeda Pharmaceutical Company Limited

350 Massachusetts Ave, Cambridge, MA 02139, USA.

Email: sandeepraj.pusalkar@takeda.com

Figure Legends

Fig. 1. Mean time course of cumulative excretion of drug-related material in urine and feces

Fig. 2. Mean (S.D.) plasma concentration-time profiles of alisertib and total radioactivity (TRA) following a single 35 mg dose of [^{14}C]-alisertib oral solution (semilogarithmic scale)

Fig. 3. Individual patient radiochromatograms of [^{14}C]-alisertib in pooled plasma samples collected between 0–192 hours post-dose.

Fig. 4. Individual patient radiochromatograms of [^{14}C]-alisertib in pooled urine samples collected between 0–192 hours post-dose.

Fig. 5. Individual patient radiochromatograms of [^{14}C]-alisertib in pooled fecal samples collected between 0–192 hours post-dose.

Fig. 6. Proposed metabolic pathways of alisertib in humans. P=Plasma; U=Urine; F=Feces; Tr=trace (<1%); Minor =1%-10%; Major = >10% of dose administered in excreta and % of total radioactivity in plasma.

Tables

TABLE 1

Summary of metabolites of [^{14}C]-alisertib observed in 0–192 hour plasma, urine, and fecal samples following administration of a single 35 mg dose of [^{14}C]-alisertib oral solution

	Accurate *m/z* (MH+)				
Metabolites	Measured	Calculated	Ppm error	Metabolite name	Matrix
M1	695.1553	695.1551	0.288	Glucuronide conjugate	P, U
M2	505.1050	505.1073	4.55	*O*-Demethylated	P, F
M3	535.1178	535.1197	3.55	Hydroxylated	P, F
M5	535.1188	535.1197	1.68	Hydroxylated	F
M4*	535.1187	535.1197	1.87	Hydroxylated	F
M8	681.1407	681.1394	1.91	*O*-Demethylated glucuronide	U
M7	681.1403	681.1394	1.32	*O*-Demethylated glucuronide	U
M9	711.1502	711.1500	0.281	Hydroxylated glucuronide	U
M10	521.1028	521.1023	0.960	Hydroxylated *O*-demethylated	F
M11	521.1014	521.1023	1.73	Hydroxylated *O*-demethylated	F
M12	521.1029	521.1023	1.15	Hydroxylated *O*-demethylated	F

M15*	524.1028	524.1019	1.72	Oxidative deaminated	F
M6	537.1323	537.1336	2.42	Hydroxylated hydrogenated	U, F
M14*	538.1182	538.1176	1.11	Oxidative deaminated	F
M13	551.1120	551.1128	1.45	Dihydroxylated	F
Alisertib	519.1227	519.1230	0.578	N/A	P, U, F

*M4, M15 and M14 coeluted

F, feces; min, minutes; MH+, protonated metabolite; N/A, not applicable; P, plasma; RT, retention time; U, urine.

TABLE 2

Radioactive peak distributions and estimated concentrations of [^{14}C]-alisertib and its metabolites in 0–192 hour pooled plasma

Patient	Peak description	Peak (%)†	$AUC_{0–192hour}$ (nM*hr)‡	% peak/alisertib
1	Total peaks	100	–	–
	M1a (peak 1)*	2.7	3,827	13.4
	M1b (peak 2)*	4.6		
	M2	40.6	24,423	85.5
	M3	4.6	2,767	9.7
	Alisertib	47.5	28,573	100.0
2	Total peaks	100	–	–
	M1a (peak 1)*	6.9	3,240	35.5
	M1b (peak 2)*	10		
	M2	35.4	7,788	85.3
	M3	6.2	1,364	14.9
	Alisertib	41.5	9,129	100.0

3	Total peaks	100	–	–
	M1a (peak 1)*	3	3,349	19.0
	M1b (peak 2)*	8.9		
	M2	27.7	8,945	50.8
	M3	5.9	1,905	10.8
	Alisertib	54.5	17,599	100.0
Mean	M1	12.0	3,472	22.6
	M2	34.6	13,719	73.9
	M3	5.6	2,012	11.8
	Alisertib	47.8	18,434	100

*M1 was observed as 2 peaks (peak 1 and peak 2) and integrated together, as the acyl glucuronide was found to undergo isomerization/rearrangement during sample processing and was deemed to be an artifact.

†Peak (%) shown is peak area as percent of total radioactivity in 0-192 hour pooled plasma.

‡Estimated AUC values in nM*hr were calculated based on the estimated concentration, molecular weight, and time period of pooling (0–192 hours).

TABLE 3

Total radioactive peak distributions of [^{14}C]-alisertib and its metabolites in urine and feces from patients administered a single 35 mg dose of [^{14}C]-alisertib oral solution (0–192 hour samples).

	Urine (% of dose)				Feces (% of dose)				Total
Patient	1	2	3	Mean	1	2	3	Mean	
Drug or metabolite									
Unknown	0.55	0.07	0.09	0.24	–	–	–	–	0.24
M7	0.60	0.13	0.11	0.28	–	–	–	–	0.28
M9	1.23	0.49	0.27	0.66	–	–	–	–	0.66
M6	0.17	0.16	0.09	0.14	3.88	5.52	3.95	4.45	4.59
M10	–	–	–	–	2.13	0.00	1.43	1.19	1.19
M1	1.29	0.62	0.61	0.84	–	–	–	–	0.84
M5	–	–	–	–	2.89	1.44	2.33	2.22	2.22
M13	–	–	–	–	3.27	3.99	1.61	2.96	2.96
M8	0.65	0.34	0.12	0.37	–	–	–	–	0.37

M4*	–	–	–	–	–	–	–	–	–
M14*	–	–	–	–	11.11	9.76	6.63	9.17	9.17
M15*	–	–	–	–	–	–	–	–	–
M11	–	–	–	–	3.19	1.95	0.00	1.72	1.72
M3	–	–	–	–	18.86	22.25	21.34	20.82	20.82
M12	–	–	–	–	8.52	5.26	4.04	5.94	5.94
Alisertib	–	–	–	–	12.40	26.07	40.35	26.27	26.27
M2	–	–	–	–	9.81	8.15	7.89	8.62	8.62
Others	0.00	0.16	–	0.05	0.00	0.00	0.00	0.00	0.05
Total of all peaks	4.49	1.97	1.29	2.58	76.06	84.39	89.57	83.36	85.94

*Metabolites M3b (M4), M523, and M537 co-eluted and were integrated.

TABLE 4

Summary of percentages of dose and contribution towards total radioactivity of metabolites observed in urine and feces following a single 35 mg dose of [^{14}C]-alisertib oral solution

	% of dose (0–192 hours)			% of dose (extrapolated to 100% recovery)*		
	Urine	Feces	Total	Urine	Feces	Total
TRA in 0–192 hour pooled samples	2.58	83.36	85.94	3.00	97.0	100
Alisertib	0	26.27	26.27	0	30.57	30.57
M2, M3, M5 + M4 derived metabolites	1.5	57.09	58.59	1.75	66.43	68.18
M1+ unknown	1.08	0	1.08	1.26	0.00	1.26
Phase I primary oxidative metabolite distribution (breakdown)						
M5, M4 derived metabolites**	0	11.39	11.39	0.00	13.25	13.25
M2 and M3 derived metabolites†	1.5	45.7	47.2	1.75	53.18	54.92

*Percent of dose excreted over 0-192 hour post-dose was extrapolated for 100% recovery estimates.

**Contribution via M5 and M4 is overestimated as M14 and M15 co-eluted with M4. Both M14 and M15 are via M3 pathway.

†Contribution via M2 and M3 is underestimated as M14 and M15 contribution is not included. Both M14 and M15 are via M3 pathway.

N/A, not available; TRA, total radioactivity.

TABLE 5

In vitro CYP phenotyping using human cDNA expressed recombinant CYP isozyme

CYP isoenzyme	Rate, nmol/min/pmol			RAF, pmol/mg protein	Adjusted rate, nmol/min/mg	Relative percentage, %*
	M2	M3	M2 + M3			
1A2	0.571733	5.351316	5.9230	4.21	49.90	2.0
2B6	0.48664	0	0.4866	1.75	14.71	0.07
2C8	10.72844	18.30959	29.0380	2.90	168.42	6.9
2C9	6.156529	0	6.1565	7.81	96.21	3.9
2C19	9.293918	0	9.2939	1.20	22.31	0.91
2D6	0.444414	0	0.4444	1.49	14.32	0.05
3A4	155.8143	99.7317	255.55	4.14	2115.92	86.2

*Human liver rate of metabolism = 124.55 pmol/min/mg.

CYP, cytochrome P450; RAF, relative activity factor.

TABLE 6

In vitro UGT Phenotyping using human cDNA expressed recombinant UGT isozymes

UGT isozyme	**Percent Relative Enzyme Activity**
UGT1A1	10.9
UGT1A3	10.3
UGT1A4	<1
UGT1A6	<1
UGT1A7	<1
UGT1A8	78.7
UGT1A9	<1
UGT1A10	<1
UGT2B4	<1
UGT2B7	<1
UGT2B15	<1
UGT2B17	<1

UGT, uridine 5’-diphospho-glucuronosyltransferase.

TABLE 7

In vitro drug-drug interaction assays

	CYP IC_{50}, μM						
	1A2	2B6	2C8	2C9	2C19	2D6	3A4/5
Alisertib	>100	ND	16.3	>100	>100	>100	72.9
M1	>100	>100	>100	>100	>100	>100	>100
M2	>50	>50	>50	>50	>50	>50	>50

CYP, cytochrome P450; IC_{50}, 50% inhibitory concentration; ND, not determined.

TABLE 8

Human Metabolite Coverage in Preclinical Species

	Human		Rat			Dog		
Dose →	**35-mg QD[a]**		**50-mg/kg Qdx7[b]**			**1-mg/kg QDx7[b]**		
Metabolite	$AUC_{0\text{-}192h}$ nM*hr	%CV	$AUC_{0\text{-}24h}$ nM*hr	%CV	Fold Coverage	$AUC_{0\text{-}24h}$ nM*hr	%CV	Fold Coverage
M1	3472	9	10733	34	3.1	509	9	0.1
M2	13719	68	13686	55	1.0	858	44	0.1

[a] Alisertib exposure in humans after 35-mg QD oral solution as a single dose is equivalent to a single 50-mg QD tablet dose.

[b] Rats and dogs were dose 50-mg/kg or 1-mg/kg, respectively, for seven consecutive days and the plasma exposure to metabolites determined after the last dose.

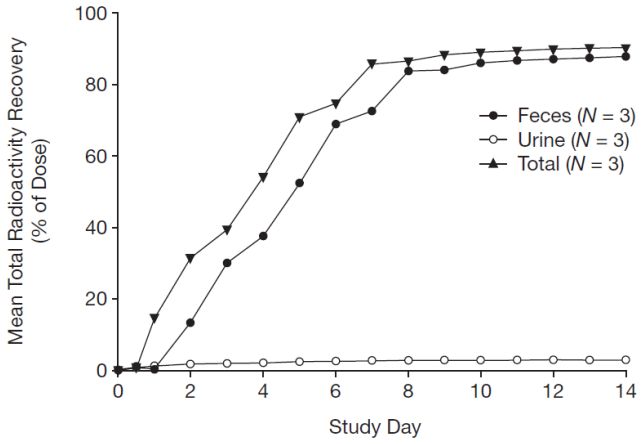

Fig. 1.

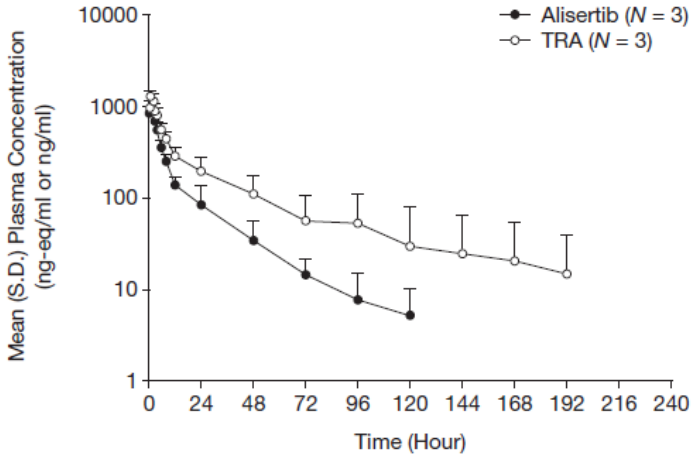

Fig. 2.

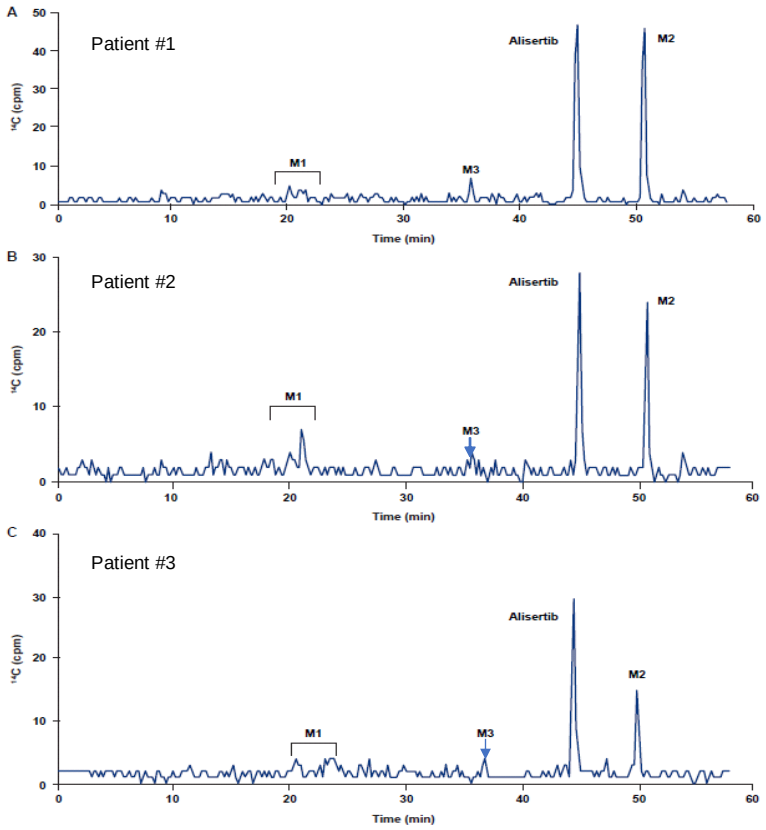

Fig. 3

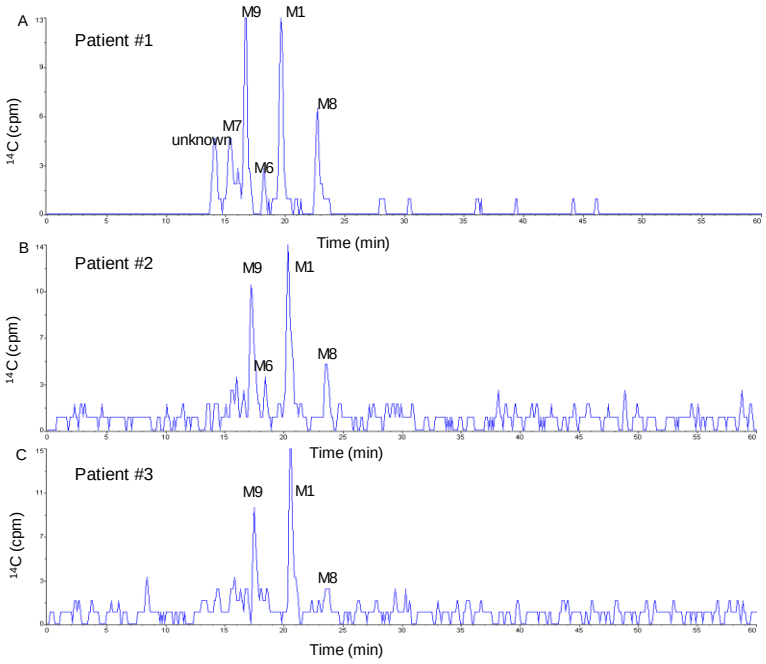

Fig. 4.

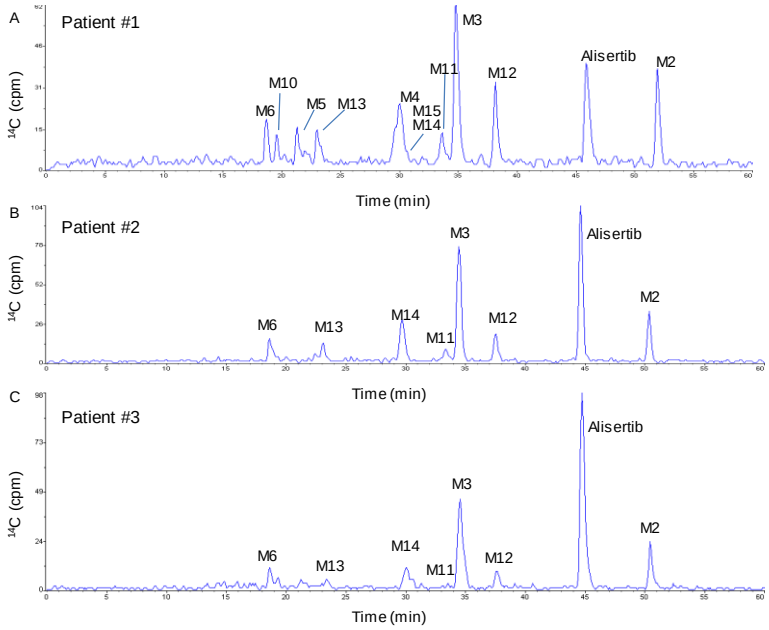

Fig. 5.

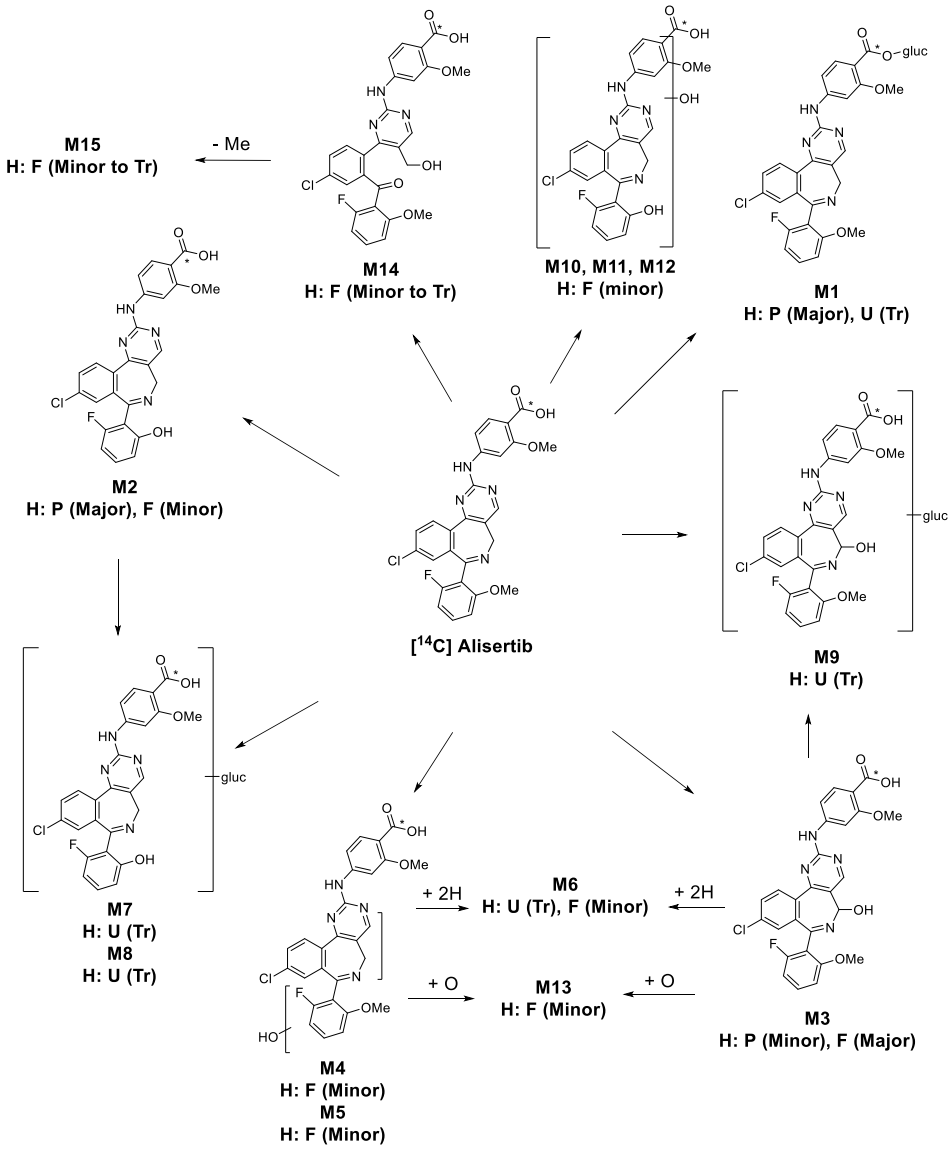

*Denotes position of ^{14}C-label.

Fig. 6.